



Impact of THz Frequency on Underwater Acoustic Wave Propagation for Short Range Wireless Applications

Md Rabiul Awal^{1,*}, Muhammad Syarifuddin Yahya¹, Nurafnida Afrizal¹, Ahmad Zaki Annuar¹, Wan Hafiza Wan Hassan¹

¹ Faculty of Ocean Engineering, Technology and Informatics, Universiti Malaysia Terengganu (UMT), 21030 Kuala Nerus, Terengganu, Malaysia

ARTICLE INFO

Article history:

Received 25 June 2021

Received in revised form 20 October 2021

Accepted 22 October 2021

Available online 21 November 2021

Keywords:

Acoustic wave propagation; ZnO;
Seawater Medium; Impedance
Mismatch; Finite Element Analysis

ABSTRACT

Acoustic propagation in seawater is an important aspect of scientific investigation. However, the impact of the THz scale frequencies for acoustic propagation is not included in the studies. Thus, a finite element analysis of such propagation in a seawater medium is presented in this paper applying THz frequencies. A transmitter (circular with a diameter of 14 mm, a thickness of 3 mm) and a rectangular receiver (20×10×0.5 mm³) are designed to trace the variations in the propagation mediums. A propagation medium of seawater (70×40×60 mm³) with ice and softwood is modelled. A scale of frequencies (1 kHz to 1 THz) is applied to trace the impact on the propagation pattern. It is found that THz range frequencies provide a very small wavelength. As a result, the potential propagation distance is very small. As such, the sound pressure level, displacements of the receiver and pressure field shows very rapid drops in the magnitude. This work considers only 70 mm as propagation distance, yet the sharp decrement of performance parameters suggests that it is rather inconvenient to achieve useful efficiency using THz frequencies for acoustic propagation.

1. Introduction

Underwater wireless communication is very important for several scientific aspects. One of the most important interests is that 95% of the ocean is still unexplored. Yet, the ocean is the largest source of natural resources with billions of unknown inhabitants in it. Hence, oceanic research and explorations have the attraction from modern research and industrial agencies from all over the world. In approach, various underwater vehicles (unmanned (UUVs) and autonomous underwater vehicles (AUVs)) are widely deployed to monitor the possible energy resources, underwater environment, marine life and seafloor activities [1, 2]. As the number of these underwater vehicles or monitoring agents are growing, a vast amount of data needs to be collected as well, to filter and analyze for further decision employments of the exploration.

To establish an effective communication channel, it is required to have a stable power module. However, wired powering is not convenient for an underwater vehicle. As such, wireless powering of

* Corresponding author.

E-mail address: rabiulawal1@gmail.com (Md Rabiul Awal)

these vehicles is well desired. Among several wireless power transfer (WPT) modules, inductive, optical and acoustic WPTs are most promising for underwater WPT. However, all of them possess positive and negative remarks [3, 4]. Acoustic energy transfer (AET), unlike the aforementioned WPTs, transfers power by propagating energy like sound or vibration waves which can be converted to useful electrical energy [5, 6]. In underwater, the generation of electricity mainly depends on the acoustic wave propagations, direction and intensity. Moreover, studies on the presence of iceberg and underwater plants in the water requires further investigation. Apart from the underwater inhabitants, ice and plants can influence wave propagation as well [8-11]. Unfortunately, there is no study available to conclude the influence in this particular area. Hence, in this paper, we have designed a seawater medium with ice and softwood as obstacle mediums to address the impact on acoustic propagations.

Additionally, the application of THz frequencies for acoustic waves requires additional investigation to trace the compatibility for underwater mediums. Yet, to date, studies on the impact of THz frequencies are not available. So, to achieve this, the designs need to be operated using a wide range of frequencies. To do so, a finite element analysis of the acoustic wave propagation in a seawater medium is presented in this work. The medium is designed to consider 3 cases; case 1 as fresh seawater, case 2 for seawater with an ice block and in case 3 seawater with ice and softwood. Ice and softwood are added to compromise the presence of iceberg and seawater plants in the seawater medium. It is worthy to investigate the impact of the different medium designs with different material characteristics. Additionally, the impact of applying THz level frequencies for a given acoustic medium requires further investigation. As such, the 1 GHz to 1 THz range of frequencies are considered as one of the scopes to indicate the initial impacts before we proceed for higher THz frequencies.

The rest of the paper is organized as; Section 2 presents details of the medium design and descriptions while Section 3 presents the evaluation of the high-frequency impacts. Lastly, Section 4 concludes this paper with some prospective future agendas.

2. Modeling of Transmitter, Receiver and Mediums in Finite Element Analysis

Acoustic propagation can be analyzed under a simulated finite element environment. To do so, a transmitter and a receiver pair can be used to study the influence. As such, a transmitter and a receiver pair are designed in this study. The transmitter is a simple circular transceiver with a Zinc Oxide (ZnO) and an aluminum (Al) layer. It is 14 mm in diameter and 3 mm in thickness (thickness of Al layer is 1 mm and ZnO is 2 mm). In contrast, the receiver is a simple ZnO rectangle block with a 20×10×0.5 mm³ dimension. The reason to keep the transmitter in a circular shape is to use the benefit of the directional acoustic beams. Also, a rectangular configuration is more beneficial as a receiver [7]. The transmitter and receiver are depicted in Figure 1. Figure 1(d) illustrates the mesh generation of the design. We have applied the maximum element size of 7.35 mm whereas the maximum element size of 1.32 mm. Maximum element growth rate and curvature factors are 1.5 and 0.6 respectively. Resolution for narrow regions is set as 0.5. These settings are selected to achieve the compromise between the structure and the simulation time.

As pictured in Figure 1, we have designed the model in a simulated environment with finite elements and later evaluated it as the same. The propagating medium is defined by a 70×40×60 mm³ liquid block. A pair of a transmitter and a receiver are placed on the two boundary ends of the medium so that the vibration from the transmitter can be collected by the receiver on the other end of the medium boundary. Three types of designs are considered in this study for acoustic evaluations. The first design includes seawater only, as of the medium, which is a 70×40×60 mm³ block as depicted

in Figure 1(a). The second design split the medium into two modules of seawater and ice. Each of them has a $35 \times 40 \times 60 \text{ mm}^3$ dimension, so the actual medium dimension remains the same, as pictured in Figure 1(b). Another material, softwood, is included in the medium for the third design. This material has similar properties to underwater plants in general. That results in the medium to be distributed as $30 \times 40 \times 60 \text{ mm}^3$ for seawater, $20 \times 40 \times 60 \text{ mm}^3$ for ice and softwood each, keeping the medium to be of the same dimension. Figure 1(c) and 1(d) presents the third design and model meshing, respectively. The transmitter and receiver dimension and position remain the same for all three designs. The material descriptions of the mediums are shown in Table 1.

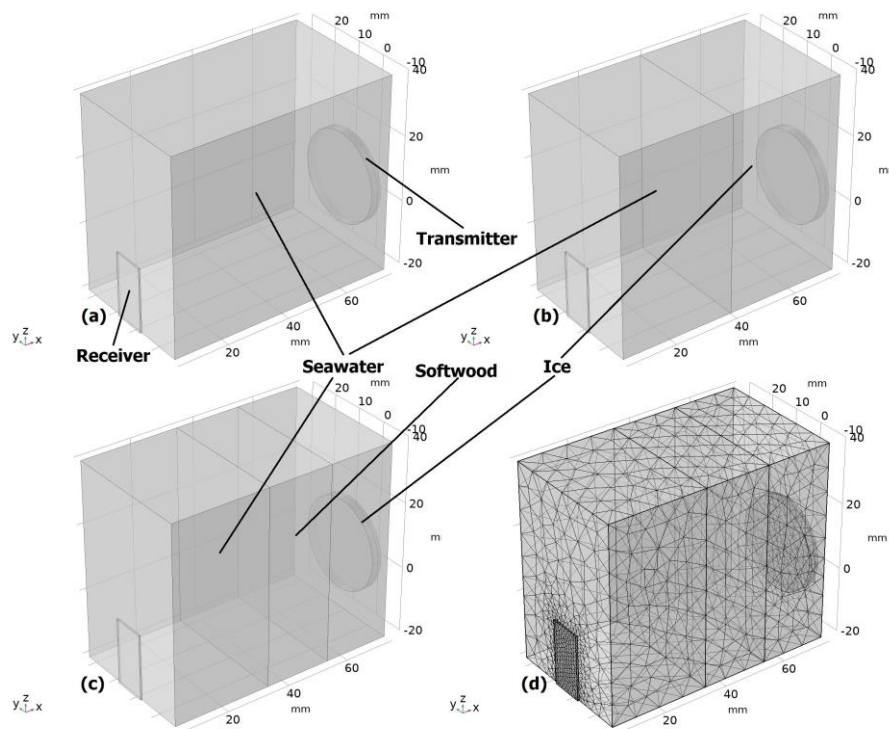


Fig. 1. Propagation medium model and mesh of (a) Seawater only, (b) Seawater and Ice, (c) Seawater, Softwood and Ice, (d) Mesh of the model

Table 1
 Medium descriptions

Medium	Dimension (mm^3)	Density (kg/m^3)	Speed of Sound (m/s)
Seawater	$70 \times 40 \times 60$	1027.3	1500
	$35 \times 40 \times 60$		
Ice	$35 \times 40 \times 60$	920	1402
	$20 \times 40 \times 60$		
Softwood	$35 \times 40 \times 60$	300	2000
	$20 \times 40 \times 60$		
Zinc Oxide	$20 \times 10 \times 0.5$	5680	6090
Aluminium		2730	6320

3. Results and Analysis of Underwater Acoustic Propagation

3.1 Sound Pressure Level

Figure 2, 3 and Table 2 explains the sound pressure level (SPL) against applied frequencies in the carrier mediums. In brief, Figure 2 informs SPL against the medium dimensions at 1 GHz and 1 THz whereas Figure 3 depicts SPL against the applied frequencies of 1 GHz to 1 THz. Table 2 summarizes

the received SPL by the receiver. From Figures 2 and 3, we can observe that the received SPL gets significantly affected by the incremental change in applied frequencies. As evident from Figures 2(a) and 2(b), the maximum and minimum SPL received at 1 GHz for the seawater medium is 72.2 dB and -82.6 dB, respectively. However, when the 1 THz frequencies are applied, the maximum and minimum SPL dropped down to 12.6 dB and -135 dB, which results in 59.9 dB and -52.4 dB SPL of difference for the 1 GHz to 1 THz range. Similarly, 72.8 dB to 12.5 dB and -80.9 dB to -129 dB SPL drop are found for the two mediums model, as in Figures 2(c) and 2(d). In relation, 74 dB to 12.8 dB and -79 dB to -132 dB SPL of difference are available for 3 mediums model as depicted in Figures 2(e) and 2(f).

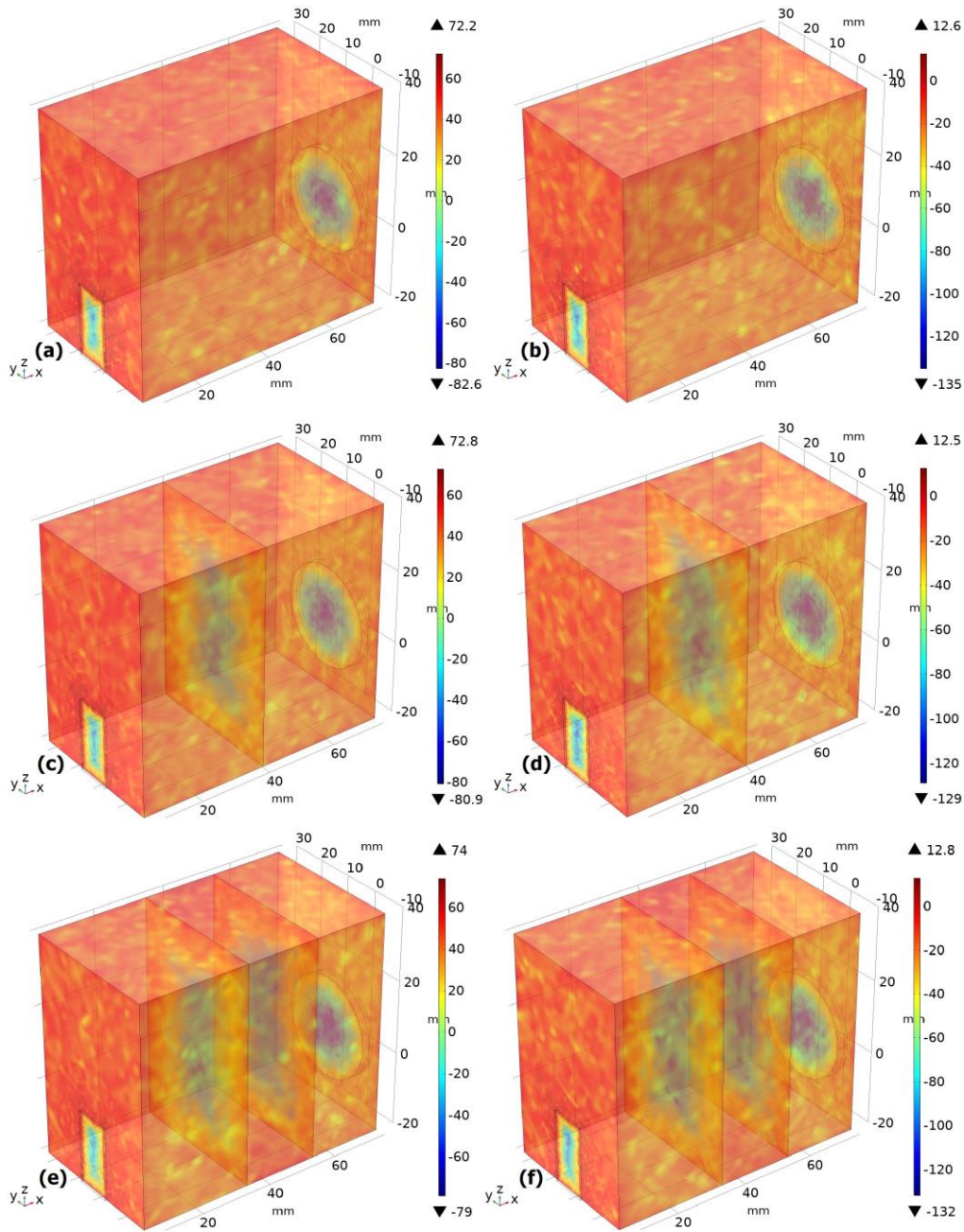


Fig. 2. Sound Pressure Level (SPL) (a) Seawater only at 1 GHz (b) Seawater only at 1 THz (c) Seawater and Ice at 1 GHz (d) Seawater and Ice at 1 THz (e) Seawater, Softwood and Ice at 1 GHz (f) Seawater, Softwood and Ice at 1 THz

A clearer pattern can be observed in Figure 3. Figures 3(a), 3(b) and 3(c) are illustrating the summarized effect of applied frequencies in single, dual and triple mediums. It is very clear from all 3 Figures that, received SPL has an inverse relationship with the applied frequencies [12, 13]. Higher frequencies result in smaller wavelengths (by applying $\lambda=v/f$ where λ is the wavelength, v is the speed of sound and f is the applied frequency). Smaller wavelengths offer lower energy density, thus, smaller propagation area. As such, rapid decrements are found in the received SPL which are provided by the higher frequencies. The summary of these findings is available in Table 2.

All figures in 2 and 3 are showing the impact of the multiple obstacles and applied frequencies on the propagation medium. When no obstacles are present in the medium, the SPL distribution is even, which follows the standard propagation pattern. However, once obstacles are added, the basic propagation (reflection, diffraction, and scattering) modes come to the picture. Hence, more added obstacles provide more disturbed propagation. This impact can be detected in Figures 2(a), 2(c) and 2(e). In addition to that, the range of frequency will determine the size of the wavelength. Higher frequencies will result in smaller wavelengths while lower frequencies result in longer wavelengths. Smaller wavelengths possess less energy density compared to longer wavelengths. Hence, smaller wavelengths restrict the propagation to a smaller area. Thus, a rapid drop in the SPL can be seen when higher frequencies are applied. These impacts are available in Figures 2(b), 2(d) and 2(f) (compared to Figures 2(a), 2(c) and 2(e)) and in Figure 3 as well.

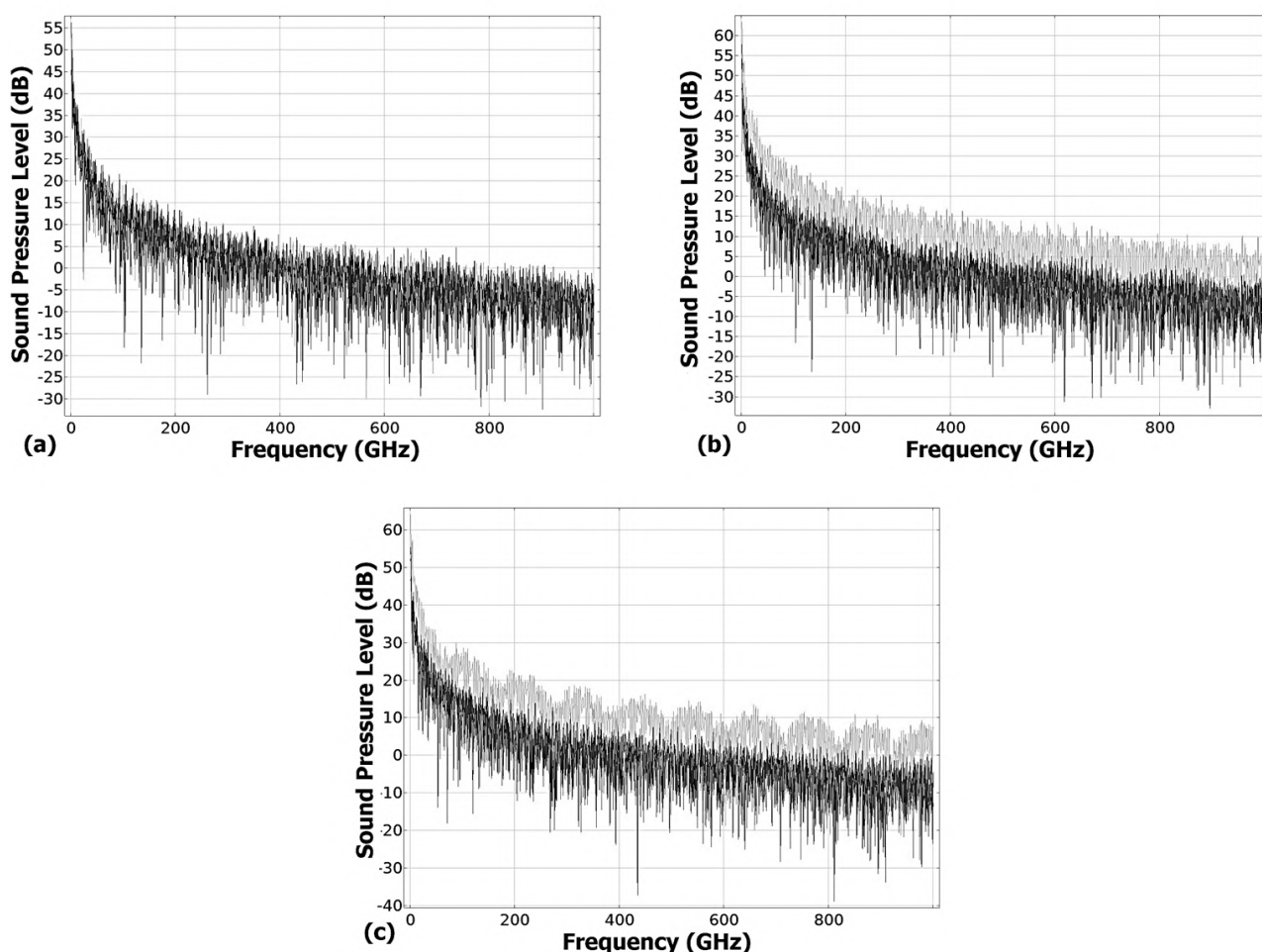


Fig. 3. Sound Pressure Level (SPL) at 1 GHz – 1 THz (a) Seawater only (b) Seawater and Ice (c) Seawater, Softwood and Ice

Table 2
 Received SPL in the layered mediums [Medium 1 (Seawater),
 Medium 2 (Seawater & Ice), Medium 1 (Seawater, Softwood & Ice)]

Medium	Max SPL (dB)	Min SPL (dB)
Medium 1	56.25 (1 GHz)	-32.4 (902 GHz)
Medium 2, layer 1	47 (1 GHz)	-64 (954 GHz)
Medium 2, layer 2	63.3 (1 GHz)	-33 (896 GHz)
Medium 3, Layer 1	55.4 (1 GHz)	-47.9 (537 GHz)
Medium 3, Layer 2	46.5 (1 GHz)	-43.1 (866 GHz)
Medium 3, Layer 3	64.1 (1 GHz)	-38.9 (811 GHz)

3.2 Displacements at the Receiver

Figure 4 and Table 3 summarize the displacement profile received by the receiver. The root means square (RMS) of displacements are presented in Figure 4 while the total displacements are shown in Figure 5. It is obvious from the figures that, increased frequencies have decreased the received displacements on the receiver. The THz frequency provides a very small wavelength, hence, the displacements are decreased as the propagated waves are losing power. Table 3 presents the summary of the RMS displacements at the receiver. From Table 3 and Figure 4 we can see that $8.38e-28$ mm displacements are found at 533 GHz whereas $9.8e-31$ mm displacements are found at 801 GHz for the seawater medium. In comparison, $1.6e-28$ mm at 502 GHz and $7e-31$ mm at 915 GHz displacements are observed for 1 GHz to 1 THz applied frequency for the dual medium of seawater and ice. The medium containing 3 materials will experience $1.93e-28$ mm at 502 GHz and $1.29e-30$ mm at 655 GHz frequencies.

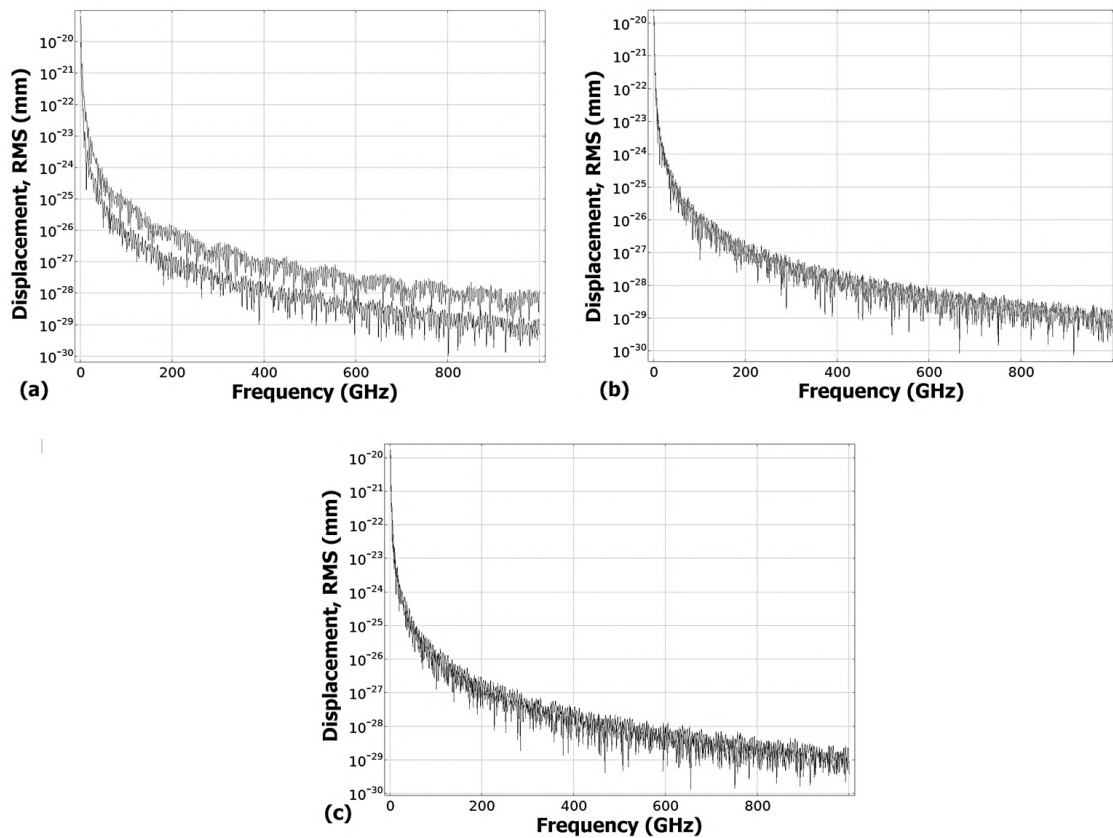


Fig. 4. Displacements RMS at 1 GHz – 1 THz (a) Seawater only (b) Seawater and Ice (c) Seawater, Softwood and Ice

Table 3

Displacements collected by the receiver [Medium 1 (Seawater), Medium 2 (Seawater & Ice), Medium 1 (Seawater, Softwood & Ice)]

Medium	Max Displacement (mm)	Min Displacement (mm)
Medium 1	8.38e-28 (533 GHz)	9.8e-31 (801 GHz)
Medium 2	1.6e-28 (502 GHz)	7e-31 (915 GHz)
Medium 3	1.93e-28 (502 GHz)	1.29e-30 (655 GHz)

Additionally, Figure 5 presents the total displacements against the applied frequencies in the reference to the arc length. A similar effect of frequencies is found as RMS displacements. It is very clear that the highest displacements are found when the lower frequencies are applied.

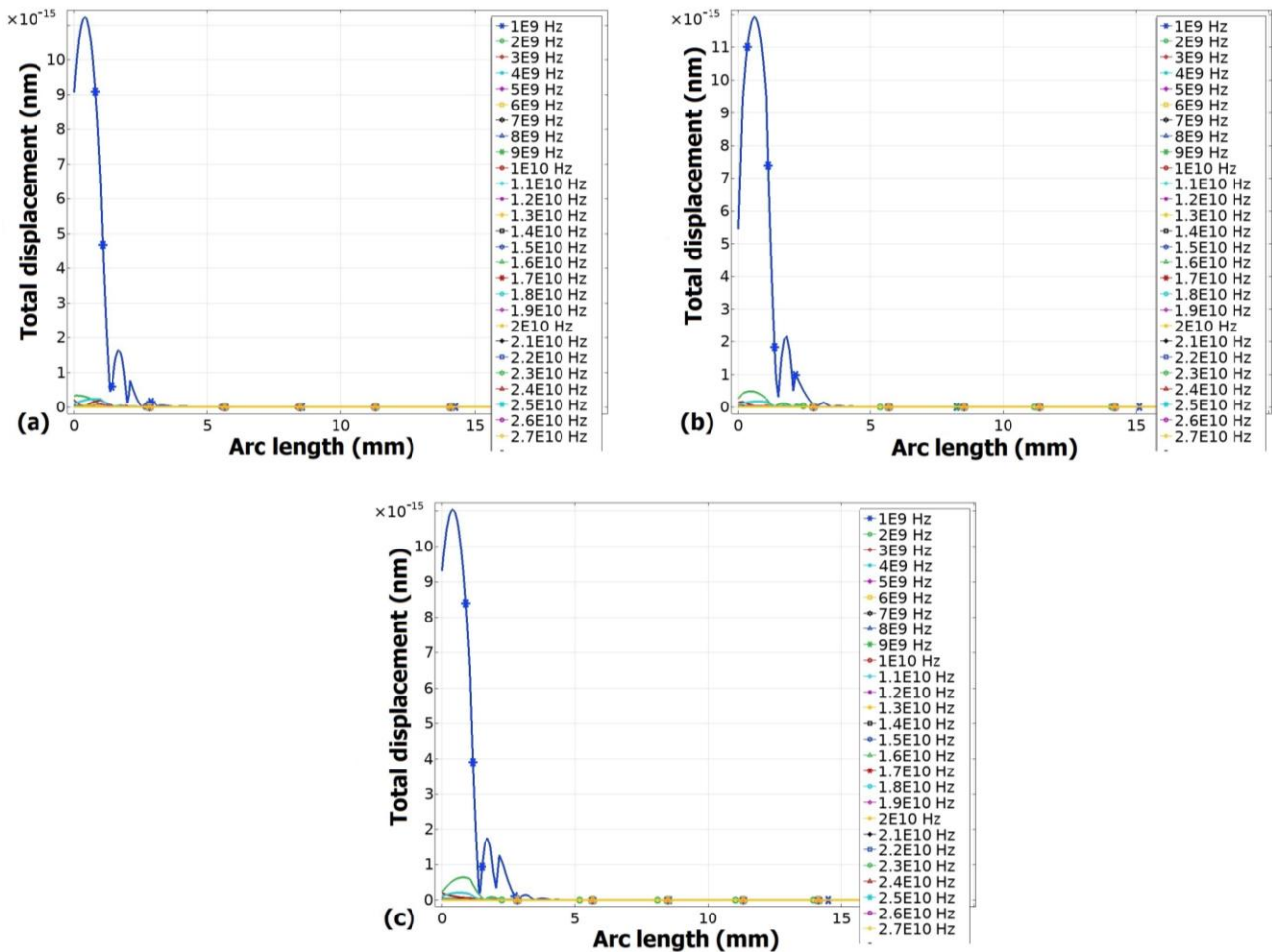


Fig. 5. Total Displacements at 1 GHz – 1 THz (a) Seawater only (b) Seawater and Ice (c) Seawater, Softwood and Ice

3.3 Acoustic Pressure Field

Figure 6 and Table 4 depict the impact of THz frequencies on an acoustic medium in the context of acoustic pressure field (APF). It is evident from the figure that, a maximum of 0.4 μPa APF is observed with the applied frequency of 3 GHz at the receiving boundary. Again, 1.7e-7 μPa is found at 552 GHz which is minimum for the single medium model. A similar impact is found when the medium includes both seawater and ice material properties, as referred to as medium 2 in Table 4.

From the table, we can see that a maximum APF of $2.85e-2 \mu\text{Pa}$ (at 47 GHz) and a minimum of $6.1e-6 \mu\text{Pa}$ (at 818 GHz) APF is available. However, when 3 materials are added to the propagation medium, the found APF seems to be closer to the seawater medium impacts. In fact, a maximum of $0.3 \mu\text{Pa}$ APF is observed at 3 GHz whereas a minimum of $2.64e-5 \mu\text{Pa}$ is found at 795 GHz of the applied frequency. The generalized descriptions are provided as in Figure 6.

Table 4

Total Acoustic Pressure Field (APF) on the receiver [Medium 1 (Seawater), Medium 2 (Seawater & Ice), Medium 1 (Seawater, Softwood & Ice)]

Medium	Max APF (μPa)	Min APF (μPa)
Medium 1	0.4 (3 GHz)	$1.74e-7$ (552 GHz)
Medium 2	$2.85e-2$ (47 GHz)	$6.1e-6$ (818 GHz)
Medium 3	0.3 (3 GHz)	$2.64e-5$ (795 GHz)

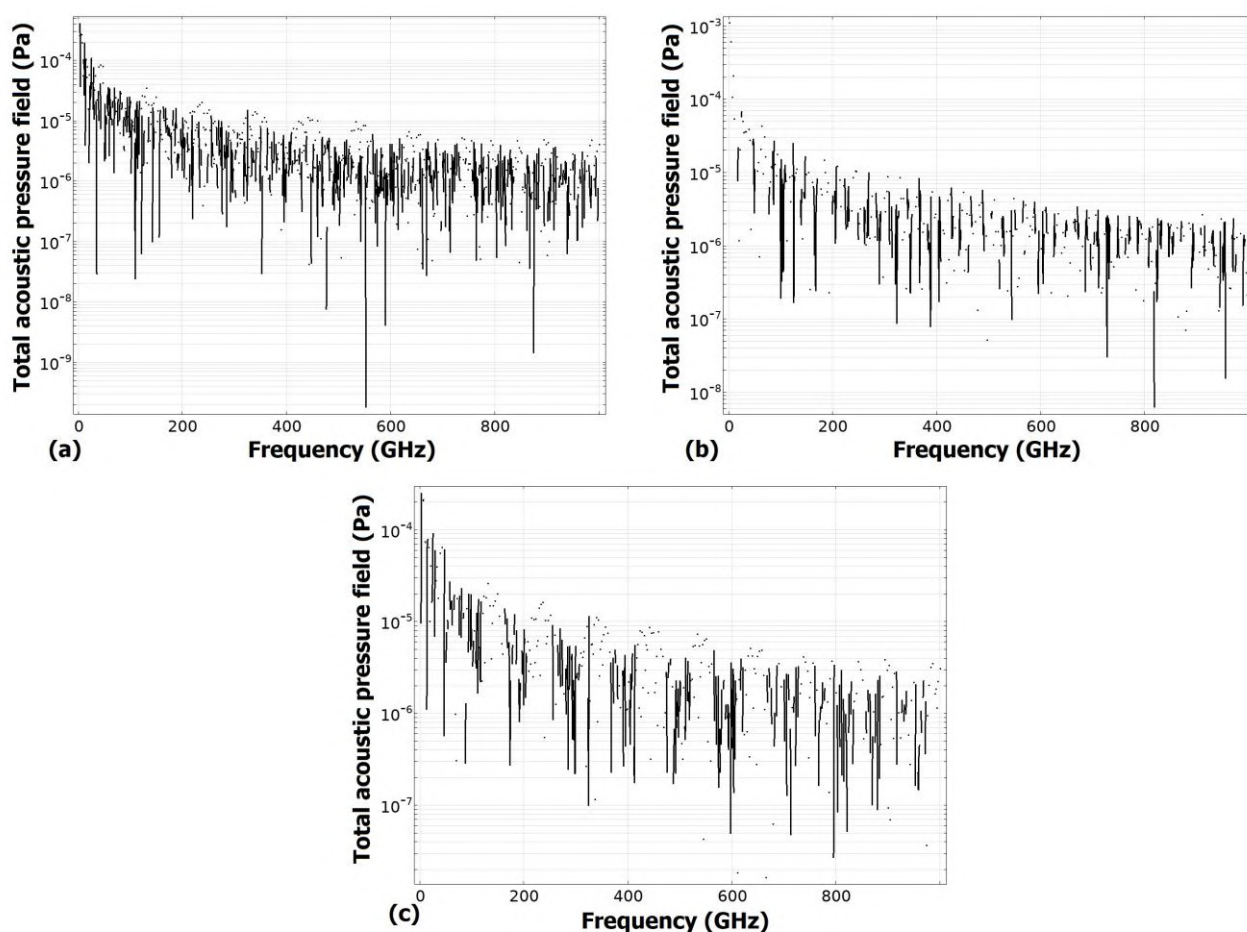


Fig. 6. Total Acoustic Pressure Field at 1GHz to 1 THz (a) Seawater only (b) Seawater and Ice (c) Seawater, Softwood and Ice

In summary, the received SPL can vary from as low as -32.4 dB (at 902 GHz, max 56.25 dB at 1 GHz) for seawater, -64 dB (at 954 GHz, max 63.3 dB at 1 GHz); for seawater with ice and -47.9 dB (at 537 GHz, max 64.1 dB at 1 GHz); and for seawater with ice and softwood. Hence, the SPL distribution is linearly decremental with the applied frequencies. The RMS displacements in the receiver are found to be a maximum of $8.38e-28 \text{ mm}$ (at 533 GHz) and a minimum of $9.8e-31 \text{ mm}$ (at 801 GHz) for seawater medium. Acoustic pressure fields (APF) found to be lies within the μPa range. In fact,

maximum APF found for the medium 1, 0.4 μPa at 3 GHz while it also shows a significant drop to $1.74\text{e-}7$ μPa at 552 GHz. A closer pattern is found for the triple medium with 0.3 μPa at 3 GHz and minimum APF of $2.64\text{e-}5$ μPa at 795 GHz. However, the worst case is found for the case of dual mediums. It exhibits a maximum APF of $2.85\text{e-}2$ μPa at 47 GHz while drops to $6.1\text{e-}6$ μPa at 818 GHz.

Now, the acoustic wavelength produced by the THz frequencies are extremely small, 0.3430 μm for 1 THz. In comparison, 343 μm wavelength for 1 GHz, and 343 mm wavelength for 1 MHz frequency. Hence, the energy density is lower for THz frequencies compared to that of MHz or even GHz frequencies [14, 15]. As a result, high frequencies seem to be suitable for near field applications only. Actually, our design considers only a 70 mm distance from the transmitter to receiver, yet, significant drops are found in SPL, APF and receiver displacements. Hence, higher energy density will be required for a longer distance (>100 m) underwater [16, 17]. This reason supports the KHz range frequencies for underwater wireless power transfer [18]. However, high frequencies can further be investigated for near field applications (<10 m) in order to estimate the guided wave and their applications [19, 20].

4. Conclusions

Finite element analysis of acoustic wave propagation with THz frequencies is evaluated in this paper. Sound pressure level (SPL), receiver displacements and acoustic pressure fields (APF) are particularly focused to trace the effect of wide-scale applied frequencies. The propagation medium considered is seawater with two added materials in it, ice and softwood. Softwood is added to the medium as the underwater plants. A set of frequencies (1 kHz - 1 THz) are applied to direct the propagation of the acoustic wave. From the results, it can be found that THz frequencies result in an extremely smaller wavelength as small as $1.5\text{e-}9$ m. This wavelength results in very weak acoustic wave propagation in seawater medium. It is found from the results that the SPL can vary from as low as -32.4 dB (at 902 GHz) to -64 dB (at 954 GHz). In addition, the SPL distribution is not linearly incremental with the applied frequencies, rather it is decremental. Similar effects are found for displacements as well. The RMS displacements in the receiver are found to be a maximum of $8.38\text{e-}28$ mm (at 533 GHz) and a minimum of $9.8\text{e-}31$ mm (at 801 GHz) for seawater medium which is very low to detect any changes. Acoustic pressure fields (APF) found to be lies within the μPa range as well. Hence, we can conclude, the increased frequency decreases the SPL and the displacements in the receiving end. It has the inverse impact on the APF too. As the displacement magnitude is the major parameter to evaluate the strength of the received power at the receiver end i.e. underwater wireless applications, it is required to be as high as possible. However, it is conclusive that, THz frequencies cannot benefit the underwater acoustic propagation for long-range. Hence, we will mainly focus on the near field acoustic propagation for future research.

Acknowledgement

This work is partially supported by Universiti Malaysia Terengganu, under fundamental research grant scheme (Ref: FRGS/1/2019/TK04/UMT/03/1), Ministry of Higher Education, Government of Malaysia.

References

- [1] Gabriel, Chadi, Mohammad-Ali Khalighi, Salah Bourennane, Pierre Léon, and Vincent Rigaud. "Monte-Carlo-based channel characterization for underwater optical communication systems." *Journal of Optical Communications and Networking* 5, no. 1 (2013): 1-12. <https://doi.org/10.1364/JOCN.5.000001>

- [2] Awan, Khalid Mahmood, Peer Azmat Shah, Khalid Iqbal, Saira Gillani, Waqas Ahmad, and Yunyoung Nam. "Underwater wireless sensor networks: A review of recent issues and challenges." *Wireless Communications and Mobile Computing* 2019 (2019). <https://doi.org/10.1155/2019/6470359>
- [3] Arvanitakis, Georgios, Jonathan McKendry, Henry T. Bookey, Erdan Gu, and Martin D. Dawson. "Light emitting diodes and lasers for high-speed underwater optical communications." *Undersea Defence Technology* (2018). <https://doi.org/10.15129/a12fc6b9-ee8d-43d8-97e7-fd22d0009468>
- [4] Jimenez, Eugenio, Gara Quintana, Pablo Mena, Pablo Dorta, Ivan Perez-Alvarez, Santiago Zazo, Marina Perez, and Eduardo Quevedo. "Investigation on radio wave propagation in shallow seawater: Simulations and measurements." In *2016 IEEE Third Underwater Communications and Networking Conference (UComms)*, pp. 1-5. IEEE, 2016. <https://doi.org/10.1109/UComms.2016.7583453>
- [5] Awal, Md Rabiul, Muzammil Jusoh, Thennarasan Sabapathy, Muhammad Ramlee Kamarudin, Hasliza A. Rahim, and Mohd Fareq Abd Malek. "Analysis of a hybrid wireless power harvester for low power applications." In *2016 10th European Conference on Antennas and Propagation (EuCAP)*, pp. 1-5. IEEE, 2016. <https://doi.org/10.1109/EuCAP.2016.7481816>
- [6] Awal, Md Rabiul, Muzammil Jusoh, Muhammad Syarifuddin Yahya, Salisa Abdul Rahman, Ahmad Nazri Dagang, Nurul Adilah Abdul Latiff, Hidayatul Aini Zakaria, and Shakir Saat. "Acoustic wave propagation in high scale impedance mismatch mediums." *IJUM Engineering Journal* 22, no. 2 (2021): 1-9. <https://doi.org/10.31436/iiumej.v22i2.1563>
- [7] Awal, Md Rabiul, Muzammil Jusoh, R. Badlishah Ahmad, Thennarasan Sabapathy, M. Najib M. Yasin, and Mohd Hafizuddin Mat. "Designing cantilever dimension for low power wireless applications." *Indones. J. Electr. Eng. Comput. Sci.* 14, no. 2 (2019): 758-764. <https://doi.org/10.11591/ijeecs.v14.i2.pp758-764>
- [8] Gao, Nansha, and Kuan Lu. "An underwater metamaterial for broadband acoustic absorption at low frequency." *Applied Acoustics* 169 (2020): 107500. <https://doi.org/10.1016/j.apacoust.2020.107500>
- [9] López-Fernández, Jesús, Unai Fernández-Plazaola, and Jose F. Paris. "Capacity estimation of the very short-range electromagnetic underwater channel based on measurements." *International Journal of Antennas and Propagation* 2014 (2014). <https://doi.org/10.1155/2014/318421>
- [10] Burrowes, Gunilla, and Jamil Y. Khan. "Short-range underwater acoustic communication networks." *Autonomous Underwater Vehicles* (2011): 173-198. <https://doi.org/10.5772/24098>
- [11] Zanaj, Elma, Ennio Gambi, Blerina Zanaj, Devis Disha, and Nels Kola. "Underwater wireless sensor networks: Estimation of acoustic channel in shallow water." *Applied Sciences* 10, no. 18 (2020): 6393. <https://doi.org/10.3390/app10186393>
- [12] Tadesse, Semere Ayalew, and Mo Li. "Sub-optical wavelength acoustic wave modulation of integrated photonic resonators at microwave frequencies." *Nature communications* 5, no. 1 (2014): 1-7. <https://doi.org/10.1038/ncomms6402>
- [13] Bar-Ziv, Uri, Aharon Postan, and Mordechai Segev. "Observation of shape-preserving accelerating underwater acoustic beams." *Physical Review B* 92, no. 10 (2015): 100301. <https://doi.org/10.1103/PhysRevB.92.100301>
- [14] Wong, Kainam Thomas, and Hoiming Chu. "Beam patterns of an underwater acoustic vector hydrophone located away from any reflecting boundary." *IEEE Journal of Oceanic Engineering* 27, no. 3 (2002): 628-637. <https://doi.org/10.1109/JOE.2002.1040945>
- [15] Beron-Vera, Francisco J., and Michael G. Brown. "Underwater acoustic beam dynamics." *The Journal of the Acoustical Society of America* 126, no. 1 (2009): 80-91. <https://doi.org/10.1121/1.3139901>
- [16] Xue, Bin, Zhiyang Wang, Kai Zhang, Haoyun Zhang, Yang Chen, Lecheng Jia, Hanzhong Wu, and Jingsheng Zhai. "Direct measurement of the sound velocity in seawater based on the pulsed acousto-optic effect between the frequency comb and the ultrasonic pulse." *Optics express* 26, no. 17 (2018): 21849-21860. <https://doi.org/10.1364/OE.26.021849>
- [17] Neighbors III, T. H. "Absorption of Sound in Seawater." In *Applied Underwater Acoustics*, pp. 273-295. Elsevier, 2017. <https://doi.org/10.1016/B978-0-12-811240-3.00004-7>
- [18] Li, Nansong, Hanhao Zhu, Xiaohan Wang, Rui Xiao, Yangyang Xue, and Guangxue Zheng. "Characteristics of Very Low Frequency Sound Propagation in Full Waveguides of Shallow Water." *Sensors* 21, no. 1 (2021): 192. <https://doi.org/10.3390/s21010192>
- [19] Hayytov, Serdar, Wah Yen Tey, Hooi Siang Kang, Mohammed W. Muhieddeen, and Omid Afshar. "Comparative Review on Computational Performance of Multistep Schemes in Solving One-Dimensional Linear Wave Equation." *CFD Letters* 13, no. 6 (2021): 1-14. <https://doi.org/10.37934/cfdl.13.6.114>
- [20] Azman, Azraf, Mohd Zamri Yusoff, Azfarizal Mukhtar, Prem Gunnasegaran, Nasri A. Hamid, and Ng Khai Ching. "Numerical Study of Heat Transfer Enhancement for Mono and Hybrid Nanofluids Flow in a Straight Pipe." *CFD Letters* 13, no. 2 (2021): 49-61. <https://doi.org/10.37934/cfdl.13.2.4961>